ISSN 1063-7761, Journal of Experimental and Theoretical Physics, 2014, Vol. 118, No. 4, pp. 611–620. © Pleiades Publishing, Inc., 2014.
Original Russian Text © E.A. Popova, S.A. Klimin, M.N. Popova, R. Klingeler, N. Tristan, B. Büchner, A.N. Vasil'ev, 2014, published in Zhurnal Eksperimental'noi i Teoreticheskoi Fiziki, 2014, Vol. 145, No. 4, pp. 697–708.

ORDER, DISORDER, AND PHASE TRANSITION IN CONDENSED SYSTEM

# Behavior of the Magnetic Subsystems in $Nd_2BaNiO_5$

**E. A. Popova[a,*], S. A. Klimin[b], M. N. Popova[b], R. Klingeler[c], N. Tristan[d], B. Büchner[d], and A. N. Vasil'ev[e]**

[a] *National Research University Higher School of Economics, Moscow, 109028 Russia*
**e-mail: eapopova@yahoo.com*
[b] *Institute of Spectroscopy, Russian Academy of Sciences, Troitsk, Moscow, 142190 Russia*
[c] *Kirchhoff Institute for Physics, University of Heidelberg, Heidelberg, INF 227 69120, Germany*
[d] *Leibniz-Institute for Solid State and Materials Research, IFW Dresden, 01171 Germany*
[e] *Moscow State University, Moscow, 119992 Russia;*
*Theoretical Physics and Applied Mathematics Department, Ural Federal University, Yekaterinburg, 620002 Russia*

Received June 21, 2013

**Abstract**—The temperature dependences of the heat capacity, the magnetic susceptibility, and the splitting of the ground Kramers doublet of the $Nd^{3+}$ ion in the chain magnet $Nd_2BaNiO_5$ are studied. An antiferromagnetic phase transition manifests itself as anomalies in all these dependences. The parameters of the Nd–Ni and Nd–Nd interactions are estimated. The field dependence of the magnetization has two anomalies. A strong magnetic anisotropy prevents the magnetic moments of the $Nd^{3+}$ ion from deviating from axis $c$ in the crystal even in an external magnetic field. The processes of magnetization and the internal specific features of a chain of spins $S = 1$ are discussed.

**DOI:** 10.1134/S1063776114030169

## INTRODUCTION

Interest in isostructural compounds with the general formula $R_2BaNiO_5$ (R is a rare-earth or yttrium ion) is caused by a substantially one-dimensional character of their magnetic properties. Slightly oblate $NiO_6$ octahedra in the crystal structure of $R_2BaNiO_5$ (space group *Immm*) join each other through apical oxygen and form chains directed along crystallographic axis $a$, which makes it possible to speak about $S(Ni^{2+}) = 1$ spin chains. These chains have no common oxygen ions and $R^{3+}$ and $Ba^{2+}$ ions are located between them [1]. $R^{3+}$ ions interact with $Ni^{2+}$ ions through the oxygen ions of the $NiO_6$ octahedra. The compound $Y_2BaNiO_5$ is a typical Haldane system with a spin gap of about 10 meV in the spectrum of magnetic excitations [2–4]. This compound does not exhibit magnetic ordering down to a temperature of at least 100 mK [4]. Complete or partial substitution of rare-earth magnetic ion $R^{3+}$ for ion $Y^{3+}$ leads to antiferromagnetic ordering. The Néel temperature of the $R_2BaNiO_5$ compounds is in the range from 12 K (R = Tm) to 65 K (R = Tb) [5–15]. Elastic neutron scattering shows that the magnetic structures of the rare-earth and nickel subsystems in the ordered state are characterized by the same wavevector $\mathbf{k} = (1/2, 0, 1/2)$ [11–13]. The orientation of magnetic moments with respect to the crystallographic axes is determined by the anisotropy of a rare-earth ion [13–15]. Inelastic neutron scattering shows that the Haldane gap in the spectrum of magnetic excitations of nickel is retained in both the paramagnetic region and the ordered state.

Thus, the paradoxical coexistence of the Haldane phase and spin waves is observed in the ordered state [16–18]. In this situation, it is incompletely clear how the nickel subsystem behaves during the measurement of the thermodynamic characteristics—either as a classical antiferromagnet with anisotropic behavior of magnetic properties or as a Haldane system with an isotropic exponential tendency toward zero magnetic susceptibility at $T \longrightarrow 0$. The specific features of the Haldane system in $R_2BaNiO_5$ can manifest themselves in the low-temperature region, just as they were revealed during theoretical and experimental investigations of doped $Y_2BaNiO_5$. Nonmagnetic impurities $Zn^{2+}$ and $Mg^{2+}$, which substitute for nickel, form direct breaks in the chains. EPR [19, 20] and NMR [21] studies showed that uncompensated spins $S = 1/2$ appear at the ends of chain segments. Impurity $Ca^{2+}$ occupies the position of $Y^{3+}$ and leads to the formation of holes in the chains and new magnetic states inside the Haldane gap [22, 23].

The purpose of this work is to study the magnetic properties of neodymium nickelate $Nd_2BaNiO_5$ from the results of investigation of its magnetization, heat capacity, and the spectroscopy of the $f$–$f$ transitions in the $Nd^{3+}$ ion. Based on the spectroscopic data, we determined the contribution of the neodymium subsystem to the heat capacity and the temperature and field dependences of magnetization. The processes of

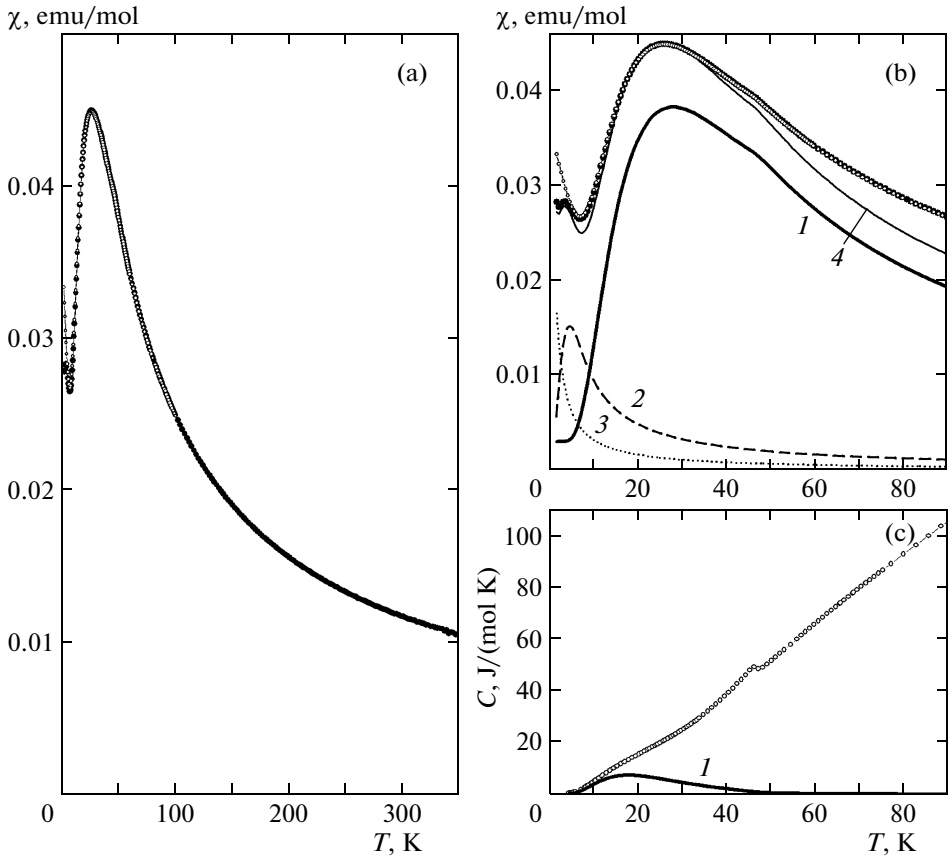


**Fig. 1.** Temperature dependences of (a, b) magnetic susceptibility of $Nd_2BaNiO_5$ measured in a field $B = 0.01$ T in (●) ZFC and (○) FC regimes and (c) heat capacity at $B = 0$. The experimental data are represented by symbols and the calculated results are represented by lines: (*1*) contributions of the neodymium subsystem to (b) magnetic susceptibility and (c) heat capacity, (*2*) contribution of the nickel subsystem related to nickel chain defects (see text), (*3*) contribution of paramagnetic impurities, and (*4*) resulting contribution of paramagnetic impurities, as well as the neodymium and nickel subsystems to the magnetic susceptibility.

magnetization and the manifestation of the internal specific features of chains of spins $S = 1$ are discussed.

## EXPERIMENTAL

Polycrystalline $Nd_2BaNiO_5$ samples were prepared by solid-phase synthesis according to the procedure described in [10]. The quality and composition of the samples were controlled by X-ray diffraction. The temperature dependences of magnetization upon field cooling (FC) and zero-field cooling (ZFC) were obtained with an MPMS-XL5 SQUID (Quantum Design) magnetometer in a magnetic field of 0.01 T and the temperature range 1.8–350 K. The temperature dependence of heat capacity in the temperature range 5–300 K in the absence of an external magnetic field was measured using a TERMIS relaxation microcalorimeter. The field dependences of magnetization in a field up to 15 T at various temperatures were measured with a vibrating-sample magnetometer, and the sweep speed of the magnetic field of the magnetometer was 0.2 T/min [24]. The measurements in fields up to 50 T were performed on a pulsed magnetometer with a pulse duration of 0.05 s. The optical measurements in the spectral region 10 000–15 000 $cm^{-1}$ and the temperature range 4.2–300 K were carried out using a BOMEM DA3.002 Fourier spectrometer.

## EXPERIMENTAL RESULTS

Figures 1a and 1b show the temperature dependences of magnetic susceptibility $\chi = M/B$ measured in a field $B = 0.01$ T in the ZFC and FC regimes. The temperature dependence of heat capacity is shown in Fig. 1c. The magnetic susceptibility at high temperatures is described by the Curie–Weiss law. The λ anomaly in the $C(T)$ dependence and the weak anomaly in the $\chi(T)$ dependence at $T_N = 47$ K indicate an antiferromagnetic phase transition. The phase-transition temperature agrees well with the data of spectroscopic [5, 14] and neutron [7] investigations. The broad maximum (Schottky anomaly) detected in the $C(T)$ and $\chi(T)$ dependences at temperatures below $T_N$ is caused by the temperature-induced electron redistribution at the sublevels of the ground Kramers doublet of the $Nd^{3+}$ ion split by the internal field appearing

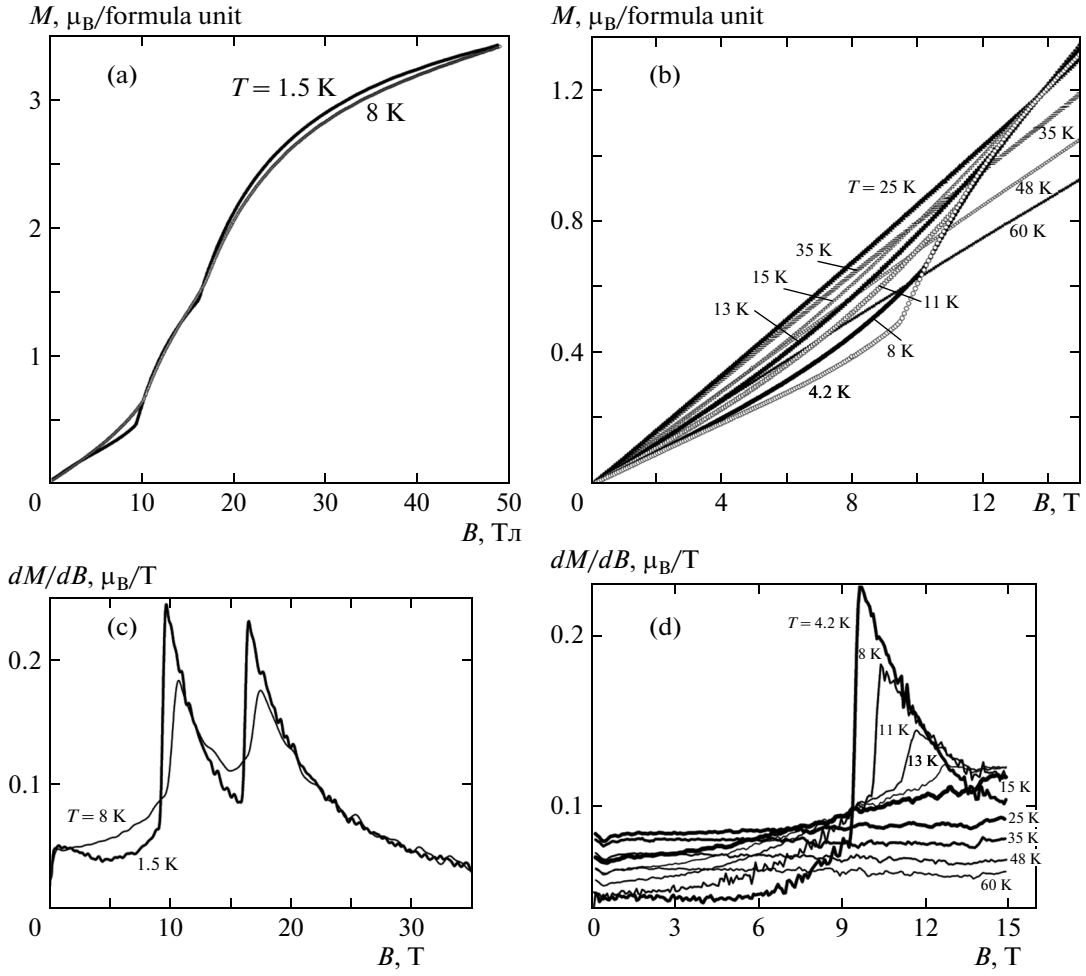


**Fig. 2.** Field dependences of (a), (b) magnetization of $Nd_2BaNiO_5$ and (c), (d) their derivatives at various temperatures.

in ordering. The $\chi(T)$ dependence measured in the ZFC regime has an additional anomaly at a temperature of about 3 K. Moreover, the behavior of the ZFC and FC magnetic susceptibilities is different in the low-temperature range, which is characteristic of a spin-glass state.

Figure 2 shows magnetization $M(B)$ and derivatives $dM/dB$ at various temperatures. At low temperatures, the $M(B)$ curves have two pronounced anomalies, namely, at field $B_{cr1} = 9.4$ T ($T = 4.2$ K) and at $B_{cr2} = 16.2$ T ($T = 4.2$ K) (Fig. 2a). Note that similar anomalies were detected in [5] at $B_{cr1} = 11$ T ($T = 4.2$ K) and $B_{cr2} = 18$ T ($T = 4.2$ K); however, their nature was not discussed. As temperature increases, the anomalies shift toward high fields. The study of the behavior of the anomaly at the first critical field ($B_{cr1}$) in the temperature range 1.5–60 K showed that this anomaly disappears at $T = 15$ K (Fig. 2b), which is significantly lower than the antiferromagnetic transition temperature ($T_N = 47$ K). This behavior is not typical of, e.g., spin-flop transition, since the shift of the critical transition field toward high fields during this spin-reorientation transition occurs up to the antiferromagnetic transition temperature.

The field dependences of magnetizations $M_a$, $M_b$, and $M_c$ measured along the crystallographic axes $a$, $b$, and $c$ in a $Nd_2BaNiO_5$ single crystal at $T = 4.2$ K were presented in [25]. These dependences are shown in Fig. 3a, which also depicts average magnetization $M = (M_a + M_b + M_c)/3$ to be compared with the results of a polycrystalline sample. A comparison of these data with the results of our experiment performed on a polycrystalline $Nd_2BaNiO_5$ sample demonstrates that the critical fields and the critical magnetizations are the same with allowance for the fact that all transitions in a real polycrystal are smooth. Note that the authors of [25] did not interpret their results. The processes of magnetization can be explained if the specific features of interaction of the magnetic subsystems in $Nd_2BaNiO_5$ are known.

We studied optical spectra to determine the contribution of the Nd subsystem to the heat capacity and to the temperature and field dependences of magnetization. Figure 4a shows the absorption spectra of

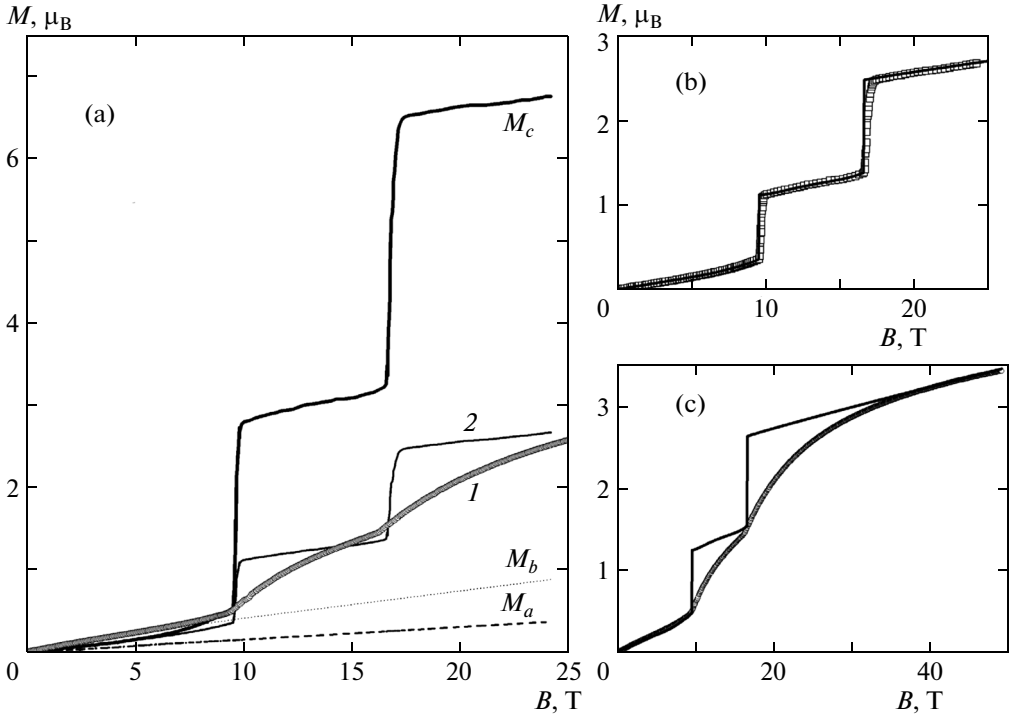


**Fig. 3.** (a) Field dependences of the magnetization of $Nd_2BaNiO_5$ at $T = 4.2$ K for (*1*) polycrystalline (this work) and single-crystal ($M_a$, $M_b$, $M_c$; [25]) samples. (*2*) Field dependence of average magnetization $M = (M_a + M_b + M_c)/3$ plotted from the experimental data for the single crystal. (b) Field dependence of $M = (M_a + M_b + M_c)/3$ plotted from experimental data for single crystal [25] (symbols) and calculation in this work (solid curve). (c) Field dependences of (symbols) magnetization of the polycrystalline sample obtained in this work and (solid curve) calculated average magnetization.

$Nd_2BaNiO_5$ at various temperatures in the range of the ${}^4I_{9/2} \longrightarrow {}^4F_{3/2}$ optical transition in the $Nd^{3+}$ ion. The ${}^4F_{3/2}$ multiplet consists of two Kramers doublets. The transition to the lowest-frequency doublet is shown. One line is detected in the paramagnetic state in this spectral region. The magnetically ordered state has four lines corresponding to transitions between the components of the split Kramers doublets. Recall that there are no perturbations except for a magnetic field (external field or internal field induced by magnetic ordering) to remove the Kramers degeneracy. Thus, the detected spectral line splitting ambiguously point to the formation of a magnetic order—it is accompanied by the appearance of an internal magnetic field at $Nd^{3+}$ ions.

## DISCUSSION OF RESULTS

The magnetic system of $Nd_2BaNiO_5$ contains two types of magnetic ions, namely, $Nd^{2+}$ ($S = 1$) and $Nd^{3+}$ ($S = 3/2$, $L = 6$, $J = 9/2$). The effective magnetic moment ($\mu_{eff} = 5.06\mu_B$, where $\mu_B$ is the Bohr magneton) estimated from the experimental data on the high-temperature ($T > 100$ K) part of the magnetic susceptibility is close to $\mu_{eff} = 5.12\mu_B$ for the free $Nd^{3+}$ ion in this compound with two neodymium ions in the formula unit. This means that nickel weakly contributes to the magnetic susceptibility in the high-temperature range. This is possible only if nickel in $Nd_2BaNiO_5$ behaves as it does in the $Y_2BaNiO_5$ Haldane system. The magnetic susceptibility of $Y_2BaNiO_5$ has a broad maximum at $T \approx 300$ K, which is characteristic of low-dimensional systems [3]. The magnetic susceptibility of $Y_2BaNiO_5$ at the maximum is $8 \times 10^{-4}$ emu/mol, which is more than an order of magnitude lower than the magnetic susceptibility of $Nd_2BaNiO_5$ at 300 K. Thus, the nickel chain in the thermodynamic measurements at $T > 100$ K behaves like a Haldane system with a gap in the spectrum of magnetic excitations. This concept agrees with the data on inelastic neutron scattering [7].

It is impossible to calculate the contribution of the nickel subsystem to the magnetic susceptibility and the heat capacity, since (as noted above) it is unclear how the Ni subsystem behaves in thermodynamic measurements because of the paradoxical coexistence of the Haldane phase and the antiferromagnetic order. Nevertheless, we estimated the contribution of the neodymium subsystem using optical experimental data.

The crystal field splits the ground state of the $Nd^{3+}$ ion (${}^4I_{9/2}$) into five Kramers doublets. The spectroscopic data demonstrate that the second Kramers doublet is higher than the ground doublet by 140 $cm^{-1}$

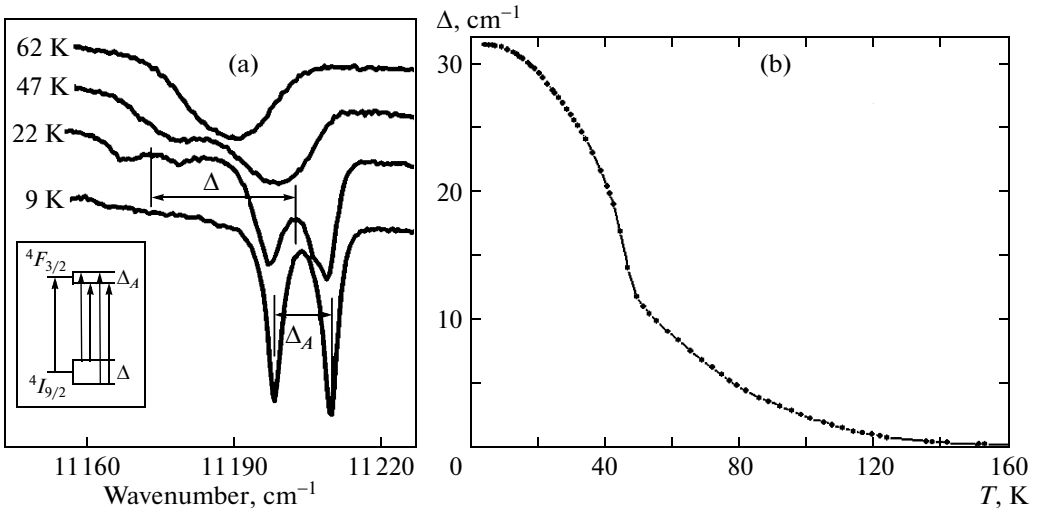


**Fig. 4.** Transmission spectra of a polycrystalline $Nd_2BaNiO_5$ sample in the range of the low-frequency line of the $^4I_{9/2} \longrightarrow {}^4F_{3/2}$ transition in the $Nd^{3+}$ ion at various temperatures (scheme in the inset explains the related transitions). (b) Temperature dependence of splitting Δ of the ground state of the $Nd^{3+}$ ion in $Nd_2BaNiO_5$.

[14]. Therefore, at temperatures below 50 K, only the ground Kramers doublet contributes to the magnetic properties of the substance. All Kramers doublets split under the action of the internal magnetic field appearing at the magnetic ordering. Each optical transition consists of four lines corresponding to transitions from the sublevels of the ground doublet to the sublevels of the excited doublet instead of one spectral line in the paramagnetic region (Fig. 4a, inset). Ground state splitting Δ was determined from the distance between the two spectral lines that correspond to transitions from the two split sublevels of the ground state of multiplet $^4I_{9/2}$ to the same sublevel of multiplet $^4F_{3/2}$. Figure 4b shows the temperature dependence of splitting Δ of the ground Kramers doublet that was obtained from the spectroscopic data. The inflection point in the $\Delta(T)$ dependence corresponds to antiferromagnetic ordering [14].

The temperature dependence of the ground Kramers doublet splitting of the $Nd^{3+}$ ion was used to estimate the contribution of the neodymium subsystem to the heat capacity and the temperature and field dependences of magnetization. According to the neutron data [7], the neodymium and nickel subsystems can be represented as two-lattice ones. In the absence of an external magnetic field, both neodymium sublattices are equivalent. The Schottky anomaly in the temperature dependence of heat capacity is caused by a change in the population of the sublevels of the ground Kramers doublet of the $Nd^{3+}$ ion, which is split by the internal magnetic field appearing in ordering. The contribution of the two neodymium sublattices is expressed as

$$C = 2R\left(\frac{\Delta}{kT}\right)^2 \frac{\exp(\Delta/kT)}{[1+\exp(\Delta/kT)]^2}, \qquad (1)$$

where $R$ is the gas constant and $k$ is the Boltzmann constant. Factor 2 indicates that two $Nd^{3+}$ ions are in the formula unit. This contribution to the total heat capacity, which is shown by the solid line in Fig. 1c, well describes the Schottky anomaly in the $C(T)$ dependence.

To calculate the contribution of the neodymium subsystem to the magnetic susceptibility, we have to take into account the fact that the neodymium sublattices become nonequivalent in an external magnetic field: the sublattice with the magnetic moment components directed along the external magnetic field is magnetized, and the other sublattice with the opposite magnetic moment directions is demagnetized. Moreover, for a correct description of the neodymium contribution to the magnetic susceptibility and magnetization, we should take into account both field $B_{ex}^{Nd}$ at the $Nd^{3+}$ ion from the side of the nickel subsystem and the interaction of the magnetic moments of $Nd^{3+}$ ions between each other. The components ($\alpha = a, b, c$) of the effective magnetic field at the $Nd^{3+}$ ions belonging to sublattices 1 and 2 are determined from the expressions [15]

$$\begin{aligned} B_{\text{eff},1\alpha} &= B_\alpha + \kappa_{11\alpha} M_{1\alpha}^{Nd} + \kappa_{12\alpha} M_{2\alpha}^{Nd} + B_{\text{ex},\alpha}^{Nd}, \\ B_{\text{eff},2\alpha} &= B_\alpha + \kappa_{11\alpha} M_{2\alpha}^{Nd} + \kappa_{12\alpha} M_{1\alpha}^{Nd} - B_{\text{ex},\alpha}^{Nd}, \end{aligned} \qquad (2)$$

where $B_\alpha$ are the external magnetic field components; $M_{1\alpha}^{Nd}$ and $M_{2\alpha}^{Nd}$ are the components of the magnetic moments of neodymium in sublattices 1 and 2, respectively; and $\kappa_{11}$ and $\kappa_{12}$ are the constants of the effective magnetic field acting on the neodymium ion from other neodymium ions having the same ($\kappa_{11}$) or the opposite ($\kappa_{12}$) magnetic moment direction. Parameter

$\kappa_{11}$ is determined by the Nd–O–Ni–O–Nd exchange interaction between the magnetic moments of two $Nd^{3+}$ ions along axis $b$ of the crystal, which occurs through the $d_{x^2-y^2}$ orbital of the $Ni^{2+}$ ion. Parameter $\kappa_{12}$ is determined by the interaction of two $Nd^{3+}$ ions having oppositely directed magnetic moments. One of the ways of the Nd–O–Ni–O–Ni–O–Nd exchange includes two $Nd^{2+}$ ions with a strong antiferromagnetic Ni–O–Ni exchange along the spin chain, and the other way passes through the apical $O^{2-}$ ion of the $NiO_6$ octahedron.

Different values of the effective field acting on $Nd^{3+}$ ions belonging to sublattices 1 and 2 result in different values of the splitting of the ground Kramers doublet of the $Nd^{3+}$ ion,

$$\Delta_{1,2} = \mu_B\sqrt{g_a^2B_{\text{eff},1,2a}^2 + g_b^2B_{\text{eff},1,2b}^2 + g_c^2B_{\text{eff},1,2c}^2}, \quad (3)$$

where $g_a = 0.36$, $g_b = 0.94$, and $g_c = 5.4$ are the components of the $g$ tensor of the ground state of the $Nd^{3+}$ ion in $Nd_2BaNiO_5$ [14]. In turn, the difference in the values of $\Delta_1$ and $\Delta_2$ leads to different magnetizations of the two neodymium sublattices. When expanding magnetic moments $M_{1\alpha}^{\text{Nd}}$ and $M_{2\alpha}^{\text{Nd}}$ of neodymium ions into a series in powers of $B_{\text{eff},1\alpha} - (B_\alpha + B_{\text{ex},\alpha}^{\text{Nd}})$ and $B_{\text{eff},2\alpha} - (B_\alpha - B_{\text{ex},\alpha}^{\text{Nd}})$ for sublattices 1 and 2, respectively, we obtain the following expressions for the magnetic moment components:

$$M_{1\alpha}^{\text{Nd}} = \frac{M_{0\alpha}^-\kappa_{12\alpha}\chi_{\alpha\alpha}^+ + M_{0\alpha}^+(1-\kappa_{11\alpha}\chi_{\alpha\alpha}^-)}{(1-\kappa_{11\alpha}\chi_{\alpha\alpha}^-)(1-\kappa_{11\alpha}\chi_{\alpha\alpha}^+) - \kappa_{12\alpha}^2\chi_{\alpha\alpha}^-\chi_{\alpha\alpha}^+}, \quad (4)$$

$$M_{2\alpha}^{\text{Nd}} = \frac{M_{0\alpha}^+\kappa_{12\alpha}\chi_{\alpha\alpha}^- + M_{0\alpha}^-(1-\kappa_{11\alpha}\chi_{\alpha\alpha}^+)}{(1-\kappa_{11\alpha}\chi_{\alpha\alpha}^-)(1-\kappa_{11\alpha}\chi_{\alpha\alpha}^+) - \kappa_{12\alpha}^2\chi_{\alpha\alpha}^-\chi_{\alpha\alpha}^+}. \quad (5)$$

Here,

$$M_{0\alpha}^\pm = 2\frac{g_\alpha^2B_{\text{eff},\alpha}\mu_B^2}{2\Delta_{1,2}}\tanh\frac{\Delta_{1,2}}{2kT},$$

$$\chi_{\alpha\alpha}^\pm = \left.\frac{\partial M_{0\alpha}^\pm}{\partial B}\right|_{\mathbf{B}_{\text{eff}} = \mathbf{B} + \mathbf{B}_{\text{ex}}}$$

are the components of the magnetic moments and the magnetic susceptibility in the effective field $\mathbf{B}_{\text{eff}} = \mathbf{B} + \mathbf{B}_{\text{ex}}$, i.e., without regard for the interaction between $Nd^{3+}$ ions. For example, if external field $\mathbf{B}$ is parallel to axis $a$, we have $B_{\text{eff},a} = B \pm B_{\text{ex},a}$, $B_{\text{eff},b} = \pm B_{\text{ex},b}$, and $B_{\text{eff},c} = \pm B_{\text{ex},c}$. Signs "+" and "–" in all these expressions belong to sublattices 1 and 2, respectively.

Formulas (4) and (5) were used to calculate the temperature dependence of the magnetic susceptibility and the field dependence of the magnetization of the neodymium subsystem when an external magnetic field is oriented along crystallographic axes $a$, $b$, and $c$. For a polycrystalline sample, the contribution of neodymium to the magnetization is determined by the expression

$$M^{\text{Nd}} = \sum_{\alpha = a,b,c}\frac{1}{3}\frac{M_{1\alpha} + M_{2\alpha}}{2},$$

and the contribution to the magnetic susceptibility is

$$\chi^{\text{Nd}} = N_A\sum_{\alpha = a,b,c}\frac{1}{3B}\frac{M_{1\alpha} + M_{2\alpha}}{2},$$

where $N_A$ is Avogadro's number.

When calculating the contribution of the neodymium subsystem to the magnetic susceptibility of $Nd_2BaNiO_5$, the temperature dependence of field $B_{\text{ex}}^{\text{Nd}}(T)$ acting from the nickel subsystem was determined from spectroscopic data using the dependence $\Delta(T)$ of the ground Kramers doublet splitting of the $Nd^{3+}$ ion. At low temperatures, we have $B_{\text{ex}}^{\text{Nd}} \approx 15.2$ T. The direction of magnetic field $\mathbf{B}_{\text{ex}}^{\text{Nd}}$ with respect to the crystallographic axes coincides with the direction of the magnetic moments of $Ni^{2+}$ ions, which lie in the $ac$ plane and deviate through an angle of 35° from axis $c$ according to the data of neutron studies [7]. The contribution of the neodymium subsystem to the magnetic susceptibility of $Nd_2BaNiO_5$ is shown in Fig. 1b by a heavy solid line. Parameters $\kappa_{11z} = -1.62$ mol/emu and $\kappa_{12z} = -1.3$ mol/emu provide a good description of the Schottky anomaly in the $\chi(T)$ dependence. The values of the other components of parameters $\kappa_{11}$ and $\kappa_{12}$ only weakly affect the calculation results, which agrees with the strong anisotropy of the magnetic properties of the compound under study. Note that if we assume $\kappa_{11} = \kappa_{12} = 0$ (i.e., if the interaction of $Nd^{3+}$ ions with each other is not taken into account), the position of the maximum in the calculated magnetic susceptibility curve is strongly shifted with respect to the maximum in the experimental curve.

With the parameters obtained, we were able to find that the magnetic moment of neodymium lies along axis $c$. This result and the determined temperature dependence of the magnetic moment of neodymium in the ordered state fully agree with the results of neutron studies in [7]. Thus, taking into account the interaction between $Nd^{3+}$ ions makes it possible to correctly describe the Schottky anomaly in the $\chi(T)$ dependence and the temperature dependence of the magnetic moment of the neodymium ion.

The contribution of the neodymium subsystem to the magnetic susceptibility of $Nd_2BaNiO_5$ does not describe the anomaly at 3 K in the ZFC $\chi(T)$ dependence. Such anomalies but at lower temperatures were detected in the weakly doped $Y_2BaNiO_5$ Haldane system. For example, in the case of substitution of $Ca^{2+}$ for $Y^{3+}$, the difference in the behaviors of the ZFC and FC magnetic susceptibilities and the shift of the max-

imum in the ac susceptibility (magnetic susceptibility in an ac magnetic field) induced by a change in frequency indicate a spin-glass state [26]. When $Ni^{2+}$ is replaced by nonmagnetic impurity $Zn^{2+}$ or $Mg^{2+}$, the position of the maximum in the ac susceptibility is frequency-independent [27]. The presence of impurities, including uncontrollable ones, in nominally pure $Y_2BaNiO_5$ causes the Schottky anomaly in the heat capacity curve, which manifests itself in an external magnetic field and shifts toward high temperatures as the field increases [28, 29].

We tried to explain the anomalies in the $\chi(T)$ dependence that were detected in our experiment at low temperatures by analogy with the explanations proposed in the works studying doped $Y_2BaNiO_5$. As in Ca-doped $Y_2BaNiO_5$, small oxygen nonstoichiometry in $Nd_2BaNiO_5$ can result in the formation of a hole in the $2p$ orbital of oxygen along a nickel chain. The competition between the antiferromagnetic and ferromagnetic exchanges that appear between neighboring nickel ions leads to a spin-glass state. It is difficult to calculate the contribution related to formation of a hole in the $2p$ orbital of oxygen inside a nickel chain. However, a comparison of the experimental data on heat capacity for $Y_{1.088}Ca_{0.012}BaNiO_5$ and $Y_2BaNi_{0.96}Mg_{0.04}O_5$ [29] shows that different types of defects, namely, holes in the $2p$ orbital of oxygen and the breaks in chains caused by the substitution nonmagnetic impurities for $Ni^{2+}$ ions, lead to the Schottky anomaly at the same temperature and that this anomaly is approximately twice as large as that in the case of a hole at the same defect concentration. We take into account this fact, calculate the contribution induced breaks in chains, simulate our experimental $\chi(T)$ dependence, and estimate the chain defect concentration in our sample (which will be discussed below in detail).

The existence of uncontrollable nonmagnetic impurities in $Nd_2BaNiO_5$, as those in nominally pure and Zn- or Mg-doped $Y_2BaNiO_5$, can result in breaks in nickel chains and the formation of a set of chain segments of various lengths. The lowest-energy level of a chain segment is fourfold degenerate [20]. Uncompensated spins $S = 1/2$, which appear at the ends of chain segments according to the model developed in [30, 31], can also interact with each other along the chain through $Nd^{3+}$ ions (in our case). This interaction causes splitting of the fourfold degenerate level into singlet ($S = 0$) and triplet ($S = 1$) states, and which of the states (singlet or triplet) is a ground state depends on whether a chain segment contains an even or odd number of $Ni^{2+}$ ions [30]. The value of splitting $\delta_1$ depends on the chain segment length [20]. The splitting of triplet $\delta_2$ into two sublevels, one of which is doubly degenerate, is caused by the anisotropy of the $Ni^{2+}$ ion inside the chain. The analysis of the EPR spectroscopy data performed in [20] showed that the state with $S = 1$ splits further into three sublevels in the presence of homogeneous external magnetic field **B** directed along crystal axis $c$ (i.e., normal to the chain). Using this four-level model, we calculated the magnetization and the magnetic susceptibility of a set of nickel chain segments.

It follows from the calculation that, to explain the anomaly in the $\chi(T)$ dependence of $Nd_2BaNiO_5$ at 3 K, the splitting of the fourfold degenerate level into a singlet and a triplet should be $\delta_1 \approx 8$ K and the splitting of the triplet should be $\delta_2 \approx 1$ K. Figure 1b (curve *2*) shows the contribution of 6% nickel chain breaks. The contribution related to the formation of a hole in the $2p$ orbital of oxygen in the nickel chain is twice as large as that related to breaks in chains. Therefore, the total defect content in the nickel chain in our sample is 3–6% depending on the relation between the total number of holes and the number of breaks in the chain. This percentage of the total number of defects obtained from our simulation of the $\chi(T)$ dependence agrees with the data in [29]. To simulate the contribution of paramagnetic impurities to the magnetic susceptibility, we used the Curie law and chose the Curie constant so that the low-temperature bend up in the $\chi(T)$ dependence is well described. Note that we failed to determine the type of paramagnetic impurities, since the chosen Curie constant depends on the impurity concentration and spin. The total contribution of the neodymium subsystem, paramagnetic impurities, and nickel chain defects is shown in Fig. 1b (curve *4*). This total contribution well describes the experimental data. Thus, structural defects allowed us to reveal the internal properties of the nickel chain. The effects associated with nickel chain defects indicate that the nickel subsystem in $Nd_2BaNiO_5$ in the ordered region exhibits the properties identical to those of the disordered $Y_2BaNiO_5$ Haldane system.

Using the values of all obtained interaction parameters of the magnetic subsystems, we were able to estimate the contribution of these subsystems to the field dependence of the magnetization of $Nd_2BaNiO_5$. The magnetization processes in this compound are caused by the behavior of the magnetic subsystems in an external magnetic field. The $g$-tensor component of the $Nd^{3+}$ ion along axis $c$ ($g_c = 5.4$) is much higher than in the perpendicular directions ($g_a = 0.34$, $g_b = 0.96$) [14]. Therefore, the magnetic moments of neodymium do not deviate from axis $c$ even in an external magnetic field (at least up to 50 T). The condition of equilibrium of the magnetic moments of the $Ni^{2+}$ ion, which lie in the $ac$ plane and deviate from axis $c$ through angle $\gamma$ ($\gamma = 35°$ at $B = 0$ [7]), is determined by the magnetic field of the single-ion anisotropy of the $Ni^{2+}$ ion, which tends to rotate the magnetic moment of nickel along axis $a$, and by the joint action of external and internal field ($B_{ex}^{Ni}$) from the $Nd^{3+}$ ion.

A comparison of the experimental $M(B)$ dependences for polycrystalline (this work) and single-crystal [25] samples at $T = 4.2$ K (Fig. 3a) shows that the orientation of magnetic moments changes when an

external magnetic field is parallel to axis $c$. Therefore, we separately considered the magnetization processes when an external magnetic field is oriented along crystallographic axes $a$, $b$, or $c$. As noted above, the contribution of the neodymium subsystem to the total magnetization was estimated by Eqs. (4) and (5) using the parameters of interaction of the magnetic subsystems obtained from the estimated contribution to the temperature dependence of magnetic susceptibility $\chi(T)$.

When simulating the magnetization processes, we took into account the relation between the magnetic moments of nickel and neodymium in both sublattices. In the absence of an external magnetic field in the ordered state, the relation between the magnetic moments of nickel and neodymium is well described by the empirical expression [7]

$$M^{\mathrm{Ni}} = 1.27\arctan(1.06M^{\mathrm{Nd}}). \quad (6)$$

An external magnetic field cannot directly affect the magnetic moment of nickel. This statement follows from the assumption that the strong interaction inside the chain ($J \approx 280$ K) prevents the magnetic moments of nickel ions from rotating with respect to each other in the external field. Moreover, the magnetization of the Haldane system is zero up to the fields corresponding to the "closure" of the Haldane gap. This fact was experimentally supported for the quasi-one-dimensional $Ni(C_2H_8N_2)NiO_2ClO_4$ (NENP) system [32], where the Haldane gap is about 11 K and 17 K along and across the chain, respectively, and the critical fields are 7.5 and 11 T, respectively. The Haldane gap in $Nd_2BaNiO_5$ is significantly larger (about 115 K [7]) and the closure field is assumed to be higher than 100 T; i.e., it is significantly higher than the fields used in this work and in [25] for a single crystal. We assumed that, in an external magnetic field, relation (6) between the magnetic moments of nickel and neodymium changes because of the magnetization of a set of nickel chain segments. The change in the magnetic moment of the nickel ion that is caused by breaks in the chain can be taken into account by adding a term that is proportional to the magnetization of the set of chain segments to $M^{\mathrm{Nd}}$ in Eq. (6).

If external field **B** is parallel to axis $c$ and $B < B_{\mathrm{cr1}}$, the magnetic moments of $Ni^{2+}$ and $Nd^{3+}$ in sublattice 1 are almost unchanged, since the magnetic moments of the $Nd^{3+}$ ion in sublattice 1 are directed along the field and reach their maximum of $2.7\mu_B$ at $T = 4.2$ K. The field acting on the $Ni^{2+}$ ions in sublattice 2 created by the neodymium subsystem decreases, since the magnetic moment of neodymium $M^{\mathrm{Ni}}$ in sublattice 2 decreases with increasing external field. However, the magnetic moment $M^{\mathrm{Ni}}$ of sublattice 2 increases. This effect is caused by the fact that the splitting between the sublevels of the triplet state of chain segments increases with the external field, and the set of chain segments that appears due to breaks in the Ni chain is magnetized in this case. Note that, if angle $\gamma$ between $\mathbf{M}^{\mathrm{Ni}}$ and axis $c$ is varied, the best agreement between a calculated magnetization curve and the experimental $M_c(B)$ dependence in the range $B < B_{\mathrm{cr1}}$ is reached at a fixed position of the magnetic moments of nickel ions ($\gamma = 35°$, as for $B = 0$ [7]) up to $B_{\mathrm{cr1}}$. Our estimation shows that, in field $B = B_{\mathrm{cr1}}$, one of the sublevels of state $S = 1$ intersects with the singlet ($S = 0$). This specific feature is likely to result in a change in the orientation of the magnetic moments of nickel at $B = B_{\mathrm{cr1}}$.

At $B = B_{\mathrm{cr1}}$(field **B** is parallel to axis $c$), the magnetic moments of the $Nd^{3+}$ ion remain parallel to axis $c$, and the magnetic moments of nickel deviate from the initial position and make an angle $\gamma \approx 60°$ with axis $c$. When the magnetization processes in $Nd_2BaNiO_5$ were simulated, angle $\gamma$ was varied and the angle $\gamma \approx 60°$ provided the best description of the step height in the experimental $M_c(B)$ dependence. As the field increases further in the range $B_{\mathrm{cr1}} < B < B_{\mathrm{cr2}}$, this curve is described best of all if we assume that the magnetic moments of $Ni^{2+}$ ions rotate continuously from $\gamma \approx 60°$ (at $B = B_{\mathrm{cr1}}$) to $\gamma \approx 30°$ (at $B = B_{\mathrm{cr2}}$), with the magnetic moments of the two nickel sublattices remaining antiferromagnetically directed with respect to each other.

In this field range, the magnetic moment of the $Nd^{3+}$ ion in sublattice 2 is almost zero and weakly depends on the external field, and the magnetic moment of the $Ni^{2+}$ ion in sublattice 2 changes mainly due to the magnetization of chain segments. At $B = B_{\mathrm{cr2}} = 16.2$ T, the magnetic moments of both $Nd^{3+}$ ion sublattices are oriented along external magnetic field **B** parallel to axis $c$ (note that the field $B = B_{\mathrm{cr2}} = 16.2$ T is close to the effective exchange field acting on neodymium, $B_{\mathrm{ex}}^{\mathrm{Nd}} \approx 15.2$ T), and the magnetic moments of the $Ni^{2+}$ ion make an angle of 65° with the external field direction. At $B > B_{\mathrm{cr2}}$, the magnetic moments of the $Ni^{2+}$ ion in both sublattices become maximal due to the magnetization of chain segments. This behavior makes an additional field-independent contribution to the resulting magnetization.

If an external magnetic field is parallel to axis $b$ (or $a$), both sublattices of the neodymium and nickel subsystems are equivalent (or almost equivalent) relative to the external field. Therefore, the direction of the magnetic moments of nickel does not change sharply over the entire field range under study.

The experimental $M_\alpha(B)$ ($\alpha = a, b, c$) dependences obtained for a single crystal in [25] are well described by the total contribution of the neodymium subsystem and paramagnetic impurities (which make a field-linear contribution to the total magnetization). In Fig. 3b, we present the result of our calculation of the average magnetization $M(B) = (M_a + M_b + M_c)/3$ of the neodymium subsystem calculated by Eqs. (4) and (5) with the addition of the magnetization of paramagnetic impurities (Curie constant was chosen so that the initial tilted section in the experimental $M(B)$ curve for a single crystal is reproduced [25]). Good agreement between the calculated and experimental [25] curves is

obvious. Except for the field range $B > B_{cr2}$ (field **B** is parallel to axis *c*), the contribution of the nickel subsystem is much smaller that it could be for the antiferromagnetically ordered system. The strong antiferromagnetic exchange inside the chain ($J \approx 100$ K) prevents the magnetic moments of nickel ions from changing their directions with respect to each other in an external field. At $B > B_{cr2}$ (where field **B** is parallel to axis *c*), both sublattices of the nickel subsystem become equivalent with respect to an external field and the field from neodymium, which causes an additional contribution to the resulting magnetization.

As for our polycrystalline sample, the experimental points in some field ranges lie higher than the curve $M(B) = (M_a + M_b + M_c)/3$ plotted from the experimental data for the single crystal (Fig. 3a). This behavior can be explained by a large number of paramagnetic impurities in our sample as compared to the single crystal studied in [25]. The solid line in Fig. 3c shows the calculated dependence of average magnetization $M(B)$ for a sample with the parameters of a system of phonon modes impurities obtained in estimating the magnetic susceptibility $\chi(T)$ of our sample. The resulting calculated magnetization includes the contribution related to defects in the nickel chain with the parameters determined for $\chi(T)$. The difference between the experimental dependence obtained for the polycrystal and the dependence calculated at $B > B_{cr1}$ is explained by the presence of various external field orientations with respect to the crystallographic axes in the polycrystal. In this case, the magnetic moments of nickel can rotate, e.g., in both a field parallel to axis *a* and a field making a certain angle with axis *c*.

## CONCLUSIONS

We studied the temperature dependences of the heat capacity, the magnetic susceptibility, and the splitting of the ground Kramers doublet of the $Nd^{3+}$ ion in $Nd_2BaNiO_5$. To describe the experimental data correctly, we took into account both the action of the nickel subsystem on the $Nd^{3+}$ ion subsystem and the interaction of the magnetic moments of neodymium with each other. An analysis of the temperature dependence of the magnetic susceptibility demonstrates that the internal disordering of the nickel subsystem manifests itself in the paramagnetic region and at low temperatures. The low-temperature anomaly (at $T \approx 3$ K) in the magnetic susceptibility curve was explained by the presence of chain defects. It was shown that the specific features in the field dependence of the magnetization of a polycrystalline sample at $B_{cr1}$ and $B_{cr2}$ that were detected correspond to the pronounced steps in the $M_c(B)$ dependence measured in a field parallel to axis *c* in a $Nd_2BaNiO_5$ single crystal [25]. This character of the field dependence of magnetization is discussed. The model proposed to explain the behavior of magnetization as a function of field takes into account that (1) the strong magnetic anisotropy of the $Nd^{3+}$ ion prevents the magnetic moments of neodymium from deviating from axis *c*, even in a high external magnetic field; (2) the strong antiferromagnetic exchange inside the chain ($J \approx 280$ K) prevents the magnetic moments of nickel ions from changing their directions with respect to each other in an external field; and (3) breaks in nickel chains, which always exist in the sample because of, e.g., paramagnetic impurities, contribute to the magnetization and change the magnetic moment of the nickel ion.

## ACKNOWLEDGMENTS

This work was performed in terms of the program of basic research of the National Research University Higher School of Economics in 2013 (project no. 112) and was supported by the Russian Foundation for Basic Research (project no. 12-02-00858-a) and the program Strongly Correlated Electrons in Solids and Structures of the Department of Physical Sciences of the Russian Academy of Sciences.

## REFERENCES

1. E. García-Matres, J. L. Martínez, J. Rodríguez-Carvajal, J. A. Alonso, A. Salinas-Sánchez, and R. Saez-Puche, J. Solid State Chem. **103**, 322 (1993).
2. R. Sáez-Puche, J. M. Corondo, C. L. Otero-Díaz, and J. M. Martín-Llorente, J. Solid State Chem. **93**, 461 (1991).
3. J. Darriet and L. P. Regnault, Solid State Commun. **86**, 409 (1993).
4. K. Kojima, A. Keren, L. P. Le, G. M. Luke, B. Nachumi, W. D. Wu, Y. J. Uemura, K. Kiyono, S. Miyasaka, H. Takagi, and S. Uchida, Phys. Rev. Lett. **74**, 3471 (1995).
5. G. G. Chepurko, Z. A. Kazei, D. A. Kudrjavtsev, R. Z. Levitin, B. V. Mill, M. N. Popova, and V. V. Snegirev, Phys. Lett. A **157**, 81 (1991).
6. E. A. Popova, A. N. Vasil'ev, S. A. Klimin, M. V. Narozhnyi, and M. N. Popova, J. Exp. Theor. Phys. **111** (2), 204 (2010).
7. T. Yokoo, S. A. Raymond, A. Zheludev, S. Maslov, E. Ressouche, I. Zaliznyak, R. Erwin, M. Nakamura, and J. Akimitsu, Phys. Rev. B: Condens. Matter **58**, 14424 (1998).
8. E. García-Matres, J. L. Garcia-Muñoz, J. L. Martínez, and J. Rodríguez-Carvajal, J. Magn. Magn. Mater. **149**, 363 (1995).
9. A. Zheludev, J. M. Tranquada, T. Vogt, and D. J. Buttrey, Europhys. Lett. **35**, 385 (1996).
10. V. Sachan, D. J. Buttrey, J. M. Tranquada, and G. Shirane, Phys. Rev. B: Condens. Matter **49**, 9658 (1994).
11. J. A. Alonso, J. Amador, J. L. Martínez, I. Rasines, J. Rodríguez-Carvajal, and R. Sáez-Puche, Solid State Commun. **76**, 467 (1990).

12. E. García-Matres, J. Rodríguez-Carvajal, J L. Martínez, A. Salinas-Sánchez, and R. Sáez-Puche, Solid State Commun. **85**, 553 (1993).
13. E. García-Matres, J. L. Martínez, and J. Rodríguez-Carjaval, Eur. Phys. J. B **24**, 59 (2001).
14. M. N. Popova, S. A. Klimin, E. P. Chukalina, E. A. Romanov, B. Z. Malkin, E. Antic-Fidancev, B. V. Mill, and G. Dhalenne, Phys. Rev. B: Condens. Matter **71**, 024414 (2005).
15. M. N. Popova, S. A. Klimin, E. P. Chukalina, B. Z. Malkin, R. Z. Levitin, B. V. Mill, and E. Antic-Fidancev, Phys. Rev. B: Condens. Matter **68**, 155103 (2003).
16. A. Zheludev, J. M. Tranquada, T. Vogt, and D. J. Buttrey, Phys. Rev. B: Condens. Matter **54**, 7210 (1996).
17. S. Maslov and A. Zheludev, Phys. Rev. Lett. **80**, 5786 (1998).
18. A. Zheludev, S. Maslov, T. Yokoo, J. Akimitsu, S. Raymond, S. E. Nagler, and K. Hirota, Phys. Rev. B: Condens. Matter **61**, 11601 (2000).
19. J. Das, A. V. Mahajan, J. Bobroff, H. Alloul, F. Alet, and E. S. Sørensen, Phys. Rev. B: Condens. Matter **69**, 144404 (2004).
20. C. D. Batista, K. Hallberg, and A. A. Aligia, Phys. Rev. B: Condens. Matter **60**, R12553 (1999).
21. F. Tedoldi, R. Santachiara, and M. Horvatić, Phys. Rev. Lett. **83**, 412 (1999).
22. Z. Hu, M. Knupfer, M. Kielwein, U. K. Rößler, M. S. Golden, J. Fink, F. M. F. de Groot, T. Ito, K. Oka, and G. Kaindl, Eur. Phys. J. B **26**, 449 (2002).
23. J. F. DiTusa, S.-W. Cheong, J.-H. Park, G. Aeppli, C. Broholm, and C. T. Chen, Phys. Rev. Lett. **73**, 1857 (1994).
24. R. Klingeler, B. Büchner, K.-Y. Choi, V. Kataev, U. Ammerahl, A. Revcolevschi, and J. Schnack, Phys. Rev. B: Condens. Matter **73**, 014426 (2006).
25. S. Okubo, H. Ohta, T. Tanaka, T. Yokoo, and J. Akimitsu, Physica B (Amsterdam) **284**, 1475 (2000).
26. E. Janod, C. Payen, F.-X. Lannuzel, and K. Schoumacker, Phys. Rev. B: Condens. Matter **63**, 212406 (2001).
27. V. Villar, R. Mélin, C. Paulsen, J. Souletie, E. Janod, and C. Payen, Eur. Phys. J. B **25**, 39 (2002).
28. A. P. Ramirez, S.-W. Cheong, and M. L. Kaplan, Phys. Rev. Lett. **72**, 3108 (1994).
29. T. Ito and H. Takagi, Physica B (Amsterdam) **329–333**, 890 (2003).
30. I. Affleck, T. Kennedy, E. H. Lieb, and H. Tasaki, Phys. Rev. Lett. **59**, 799 (1987).
31. E. S. Sørensen and I. Affleck, Phys. Rev. B: Condens. Matter **49**, 15771 (1994).
32. K. Katsumata, H. Hori, T. Takeuchi, M. Date, A. Yamagishi, and J. P. Renard, Phys. Rev. Lett. **63**, 86 (1989).

*Translated by K. Shakhlevich*